

Design and Analysis Tool for Mars Atmospheric Entry Missions

Jyothish R. Pillai^a, Alex John^a and R. V. Ramanan^b

^aScientist, Vikram Sarabhai Space Centre, Thiruvananthapuram, India

^bAdjunct Professor, Department of Aerospace Engineering, Indian Institute of Space Science and Technology, Thiruvananthapuram, India

Abstract

A numerical tool is developed for the design and analysis of Mars atmospheric entry trajectories. Simple latitude dependent density model is employed along with an approximate temperature model for Mars' atmosphere. Radiative heat flux and convective heat flux (with cold wall boundary condition) relations are used for the study of stagnation point heating. Approximate drag profile of Mars Pathfinder is used for most simulations. Effects of non-spherical gravity and Mars' surface elevation considerations are discussed in brief. De-orbit thrusting, direct entry, lifting entry, parachute deployment, heat shield release and terminal descent thrusting scenarios are also incorporated into the tool, and their design characteristics are studied. Advantages of lifting entry and the necessity for parachute deployment and terminal descent thrusting are discussed. Different direct entry scenarios are analyzed within feasible launch windows for a typical Mars mission.

NOMENCLATURE AND CONSTANTS

D = Drag force on the module

I_{sp} = Specific impulse of thruster

J_2 = Zonal gravity coefficient for Mars = 0.001964

L = Lift force on the module

L/D = Lift to Drag ratio

R = Equatorial radius of Mars = 3397 km

T = Thrust force on the module

g_0 = Gravitational acceleration on Earth surface = 9.80665 m/s²

g_r = Radial component of gravity

g_ϕ = Latitudinal component of gravity

m = Mass of the module

r = Radial distance of the module from the centre of Mars

t = Time

v = Velocity of the module

α = Angle of attack of module

β = Bank angle of module

γ = Flight path angle (FPA)

δ, φ = Mars-centric latitude

λ = Mars-centric longitude (+ towards east)

μ = Gravitational constant of Mars = 42828 km³/s²

ρ = Density of atmosphere

ψ = Flight azimuth (+ clockwise from north)

ω_M = Mars rotation rate = 7.101171898 × 10⁻⁵ rad/s

Characteristic gas constant = 191.8 J/kg/K

Ratio of specific heats = 1.289

dof - Degree of Freedom

MPF - MARS PATHFINDER

1. INTRODUCTION

“The earth is the cradle of humankind, but one cannot live in the cradle forever.”

- Konstantin Tsiolkovsky

The interest in planetary exploration, mainly the exploration of Mars, has greatly increased in recent times, largely due to the advancements in space technology. So far fourteen attempts have been made by different agencies to land on the surface of the red planet. The United States has successfully landed 5 robotic systems on the Mars surface till date. These were part of Viking I and II, Pathfinder and Mars Exploration Rover (Spirit and Opportunity) missions. All these missions had landed masses below 600 kg. For further larger scale missions, the landing mass capability has to be increased to several tonnes or more [1]. Available literature points out that, entry systems with ballistic coefficients greater than 50 kg/m² cannot decelerate payloads to subsonic conditions at the Martian surface without the help of additional decelerators like supersonic parachutes, terminal descent thrusters, or airbags. These requirements and several other factors like the thin atmosphere, uneven terrain, bi-modal Mars surface elevation, high system qualification, etc. pose substantial challenges in the design of the entry module as well as its entry, descent and landing phases, which have to be addressed during the initial simulation stages. In this paper, a mission design and analysis tool for use in Mars entry mission is discussed. Analysis for critical entry design parameters is carried out. Further, using the tool, a typical entry scenario is analyzed for a Mars mission opportunity in 2013.

2. ENTRY DESIGN METHODOLOGY

The entry trajectory phases of a typical Mars entry module are as follows: i) Direct atmospheric entry starts at an altitude of 125 km above the Martian surface; ii) Parachute deployment is to occur around an altitude of 7–10 km and the desired parachute deployment Mach no. lies in the range 1.4–2.1; iii) Parachute deployment is followed by heat-shield release at a height 6.5 km above the Mars areoid. Heat-shield release decreases the overall mass of the entry body and thus brings down ballistic coefficient and hence the terminal velocity; iv) Terminal descent thrusters are to be fired at a height around 50 m above the surface for 2 s to achieve near zero velocity for soft landing.

For the 3D simulations, the equations of motion of a body under gravity, w.r.t a 3D rotating Mars is used.

$$\frac{dr}{dt} = v \sin \gamma$$

$$\frac{d\lambda}{dt} = \frac{v \cos \gamma \sin \psi}{r \cos \delta}$$

$$\frac{d\delta}{dt} = \frac{v \cos \gamma \cos \psi}{r}$$

$$\frac{dv}{dt} = \frac{T \cos \alpha - D}{m} - g_r \sin \gamma + g_\phi \cos \gamma \cos \psi + \omega_M^2 r \cos \delta (\sin \gamma \cos \delta - \sin \delta \cos \gamma \cos \psi)$$

$$\begin{aligned} \frac{d\gamma}{dt} = & \frac{v}{r} \cos \gamma + \frac{T \sin \alpha + L}{mv} \cos \beta - \frac{g_r \cos \gamma}{v} - \frac{g_\phi \sin \gamma \cos \psi}{v} + 2\omega_M \sin \psi \cos \delta \\ & + \frac{\omega_M^2 r \cos \delta}{v} \cos \psi \sin \gamma \sin \delta + \cos \gamma \cos \delta \end{aligned}$$

$$\begin{aligned} \frac{d\psi}{dt} = & \frac{v}{r} \tan \delta \sin \psi \cos \gamma + \frac{T \sin \alpha + L}{mv \cos \gamma} \sin \beta - \frac{g_\phi \sin \psi}{v \cos \gamma} + 2\omega_M (\sin \delta - \cos \psi \cos \delta \tan \gamma) \\ & + \frac{r}{v \cos \gamma} \omega_M^2 \sin \psi \cos \delta \sin \delta \end{aligned}$$

$$\frac{dm}{dt} = \frac{T}{g_0 I_{sp}}$$

Velocity appearing in these equations is the velocity of the module w.r.t Mars’ surface. Lift, drag and thrusting forces are also included. Besides, their effects are modified by angle of attack and bank angle variables.

The atmospheric density model used is referenced from “Analytical models of Mars’ atmospheric density” by L. Sehnal [2]. Out of the minimal, maximal and nominal models, only the nominal model has been used for the simulations here. The latitudinal dependence of density makes its distribution unsymmetrical about the equator.

The atmospheric temperature model for simulations is as given in [3]. Mars has a surface temperature that oscillates between 140 and 300 K. The inclination of its axis of rotation (similar to the terrestrial) and the high eccentricity of the Martian orbit induce a seasonal cycle more intense than the terrestrial one. However, neglecting these seasonal variations, a typical temperature profile is used (Figure 1).

The calculation of convective heat fluxes is carried out using the Sutton-Graves convective heating correlation [4]. This correlation calculates the cold wall heat flux at the stagnation point on the entry module (Heat flux at the stagnation point is typically the largest for the whole body). The Tauber-Sutton correlation [5] is used for the calculation of radiative heat flux at the stagnation point on the entry module.

Entry module drag coefficients do not vary greatly with Mach number, and hence using a constant drag coefficient for the entire flight regime is good enough here. However, the same is not the case with lift coefficients. Lift coefficients vary significantly with angle of attack of the entry module. Again, since full 6-dof simulations have not been performed, using a constant lift to drag ratio for the entire flight is sufficient to obtain underlying trends in trajectory simulations. In order to obtain greater accuracy in simulations, the drag coefficient profile of MPF [6], w.r.t Mach number is incorporated into the simulations (Figure 2).

Parachute deployment is a crucial stage in the entry mission. It reduces the ballistic coefficient by increasing drag and the area. The parachute model used in this project is a crude one. Here, from the instant the parachute is deployed, the drag due to parachute is simply added to the total drag of the module.

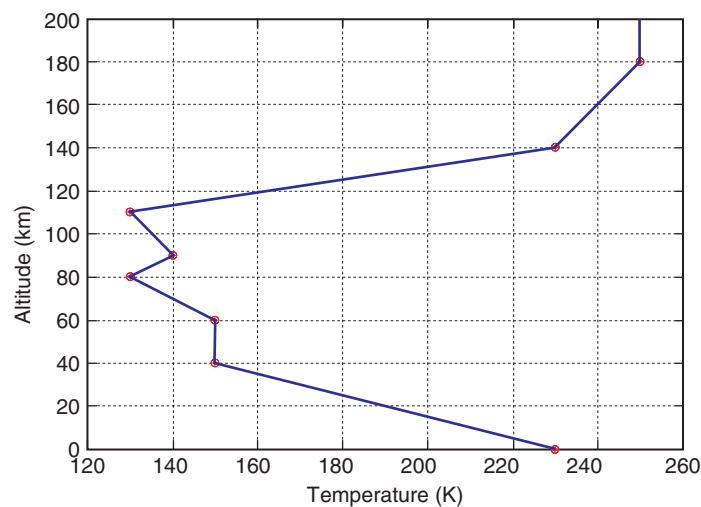


Figure 1. Typical Mars’ atmospheric temperature profile (linearly interpolated).

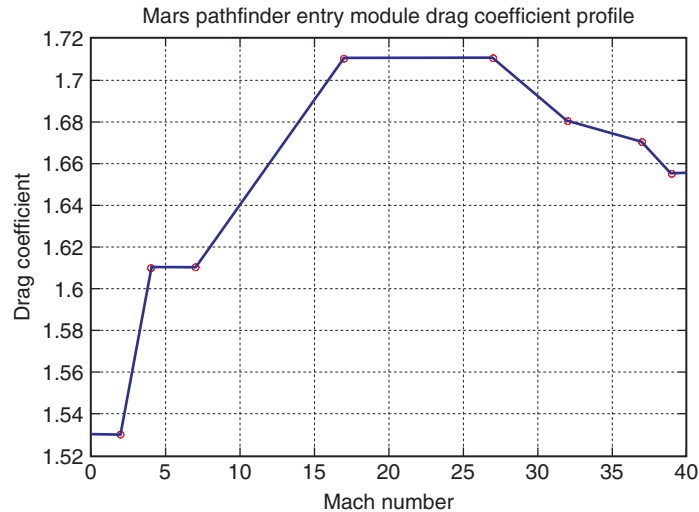


Figure 2. Drag coefficient v/s Mach number (Linearly interpolated) for MPF entry module. [6]

Terminal descent thrusters are provided to decelerate the entry body to near zero velocities, thus facilitating soft landing. These thrusters should have very high thrust levels, so that the required velocity impulse can be provided as quickly as possible. This minimizes the velocity increase due to gravity during thrusting. Moreover, the thrusting is to be started as late as possible, i.e. the last 2–4 seconds of flight, so that once the thrusting is stopped, the module will not accelerate much due to gravity during free fall. Determination of the thrust levels of the terminal descent thrusters is carried out in the following manner: (i) From the terminal velocity and the altitude (for considering velocity increase due to gravity), the velocity to be nullified is found, (ii) the propellant required and the thrust level are estimated from the rocket equation. Further refinements on thrust levels are done with iterative runs.

The shape of Mars is not exactly spherical and Mars is much more flattened at the poles than Earth. Hence, the effects of non-spherical gravitational field of Mars may be much more significant. However, since atmospheric entry trajectories typically last only about a few hundred seconds, the cumulative effects of non-spherical gravity will not contribute to any major deviations in results. In this paper, the spherical gravity model (one where gravity force acts only in the radial direction) has been used for almost all the simulations. In order to quantify the effects of non-spherical gravity, a zonal gravity model [7] is used.

$$g_r = \frac{\mu}{r^2} \left\{ 1 - \frac{3}{2} \left(\frac{R}{r} \right)^2 J_2 (3 \sin^2 \phi - 1) \right\}$$

$$g_\phi = -\frac{\mu}{r^2} \left\{ 3 \left(\frac{R}{r} \right)^2 J_2 \sin \phi \cos \phi \right\}$$

The surface of Mars is highly irregular. Almost whole of the northern hemisphere is below the Mars areoid (equivalent to Earth sea level), while the southern hemisphere is above it. Mission level entry trajectory simulations require the incorporation of the Mars elevation data so as to obtain accurate results. For this purpose, the Mars Orbiter Laser Altimeter (MOLA) topography data is utilized. This data is freely available from NASA archives [8].

Runge-Kutta 4th order integration method [9, 10] has been used for numerical integration in this paper. Almost all simulations use a time step of 0.01s, unless specified otherwise. However, all thrusting simulations are done with 0.001 s time step. This is done so as to achieve the required velocity impulse as closely as possible (i. e. to avoid overshooting).

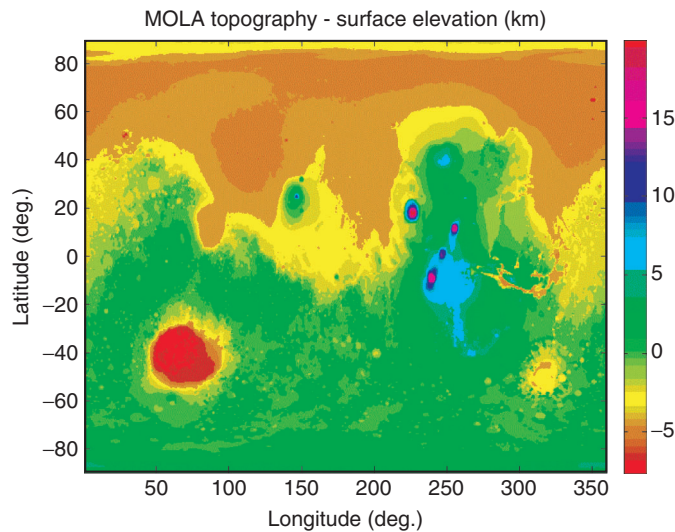


Figure 3. Mars surface elevation (generated from MOLA topography data file: resolution 0.5°).

3. RESULTS AND DISCUSSIONS

The design and analysis tool developed in C++ is used to analyze the entry scenarios and various aspects of the critical design. Typical values of the entry module properties and entry conditions are given in Table 1. Most of the values are from MPF mission. Comparison of the design parameters in various phases of the entry mission is attempted to bring out the contributions of various subsystems.

3.1. Entry design options and analysis

Table 2 clearly shows the advantages of having a lifting entry body over a ballistic entry body. The touchdown velocity, peak dynamic pressure and acceleration are lower in the case of the lifting entry case, which is desirable. Time spent in the atmosphere increases on adding lift which gives sufficient time for parachute deployment and other manoeuvres.

It is observed that the velocity of the ballistic entry body reaches a terminal value of about 210 m/s irrespective of the entry velocity. In order to reduce the touchdown velocity, the feasibility of

Table 1. Typical values of entry module and parachute properties

| Module properties | |
|-------------------------------|-----------------------|
| Reference area | 5.52 m ² |
| Lift to drag ratio | 0 |
| Initial mass | 603 kg |
| Entry/Initial conditions | |
| Radial distance | 3522.2 km |
| Longitude | 338.9036° |
| Declination | 22.984° |
| Velocity | 7350.9 m/s |
| Flight path angle | -14.2° |
| Flight azimuth | 253.0995° |
| Parachute properties | |
| Parachute drag coefficient | 0.4 |
| Reference area of parachute | 122.72 m ² |
| Parachute deployment altitude | 8.6 km |
| Heat-shield release altitude | 6.5 km |
| Heat-shield mass | 175 kg |

Table 2. Comparison of trajectory parameters for lifting and non-lifting entry simulations

| Touchdown & peak parameters | L/D = 0 | L/D = 0.1 | L/D = 0.2 |
|-------------------------------------|----------|-----------|-----------|
| Velocity (m/s) | 210.07 | 208.12 | 198.86 |
| Flight time (s) | 198.08 | 305.14 | 517.70 |
| Ground track (km) | 612.94 | 718.04 | 1102.44 |
| Peak Dynamic Pressure (Pa) | 10762.30 | 9343.14 | 8193.80 |
| Peak heat flux (W/cm ²) | 118.70 | 116.14 | 113.65 |
| Peak acceleration (in Earth g) | 17.17 | 14.91 | 13.07 |

parachute deployment, at around Mach number 2 (assumed as parachute design requirement), is studied. The nominal parachute deployment altitude is taken as 8.6 km. Further delaying the parachute deployment may not provide us the sufficient time required for the module to decelerate to near zero velocities. Table 3 presents the change in entry design scenario due to the inclusion of the parachute.

Parachute deployment decelerates the module and brings down the terminal velocity to about 70 m/s. The steeper touchdown FPA favours vertical landing and the increased time can be advantageous for the ground detection sensors and other monitors to be operational and for a more controlled landing.

Heat shield release can decrease the terminal velocity and also the ballistic coefficient of the entire module. The reduced mass of the module reduces the amount of fuel to be used in the terminal descent thrusters which is the only available option to further reduce the touchdown velocity of the module. The result from the simulation is given for a heat shield mass of 175 kg, released at an altitude of 6.5 km. It is clear that the heat-shield release further reduces the end velocity to 60 m/s and also increases the flight time (Table 4).

For the nominal simulations, the terminal velocity is around 60 m/s. To bring the velocity further down for a soft landing, terminal descent thrusters have to be used. The following data are used for the calculation of thrust levels.

- Terminal velocity of the lander \approx 60 m/s
- Altitude at which thrusting is to be started \approx 50 m (approx., from MPF data [11])

Table 3. Comparison of key trajectory parameters of the entry module with and without parachute deployment

| Touchdown parameters | W/o parachute | With parachute |
|--|---------------|----------------|
| Velocity(m/s) | 210.07 | 71.57 |
| Ground Track(km) | 612.94 | 607.20 |
| Integrated heat load(J/cm ²) | 4207.32 | 4205.05 |
| FPA(deg.) | -51.07 | -88.21 |
| Flight time(s) | 198.08 | 244.70 |

Table 4. Comparison of key trajectory parameters with and without heat-shield release

| Touchdown parameters | With Heat shield release | W/o Heat shield release |
|--|--------------------------|-------------------------|
| Velocity(m/s) | 59.75 | 71.57 |
| Ground Track(km) | 605.07 | 607.20 |
| Integrated heat load(J/cm ²) | 4204.12 | 4205.05 |
| FPA(deg.) | -89.69 | -88.21 |
| Flight time(s) | 264.01 | 244.70 |

- Velocity increase due to gravity during a 50 m free-fall ≈ 17 m/s (Actual value will be lesser, due to atmospheric drag)
- Net velocity impulse to be imparted by thrusters $\approx 60 + 17 \approx 77$ m/s

Since solid rocket motors are used, we consider an $I_{sp} = 280$ s. For the module of mass 428 kg (after heat-shield release), assuming a burn time of 2 s, we find that the thrust required is ≈ 18 kN. Using thrust values of 17 kN and 18 kN, with the burn start time and velocity impulse decided iteratively so as to obtain the lowest touchdown velocity, simulations are carried out. The results are given in Table 5. Velocity impulse decided for both cases is 64.3 m/s. These simulations show that when thrusters are ignited at around 50 m altitude, the module can reach near zero velocities in fewer than 2 s.

3.2. Entry analysis with non-spherical gravity

The zonal gravity model [7], described in an earlier section has been used in two simulations and the results are compared in Table 6, with the results obtained using spherical gravity model.

It is now clear that the effect of non-spherical gravity is in fact negligible in entry trajectory simulation. The only major deviation that occurs is in the touchdown flight azimuth angle. Similar trends are observed in higher altitudes also.

3.3. Entry analysis including Mars topography data

Two simulations are performed that includes the Mars topography data [8]. One of them corresponds to the nominal entry conditions and in the other one the entry latitude and longitude are changed to -22.984° and 310° respectively. The latter simulation hence starts and ends in the southern hemisphere. The specific value of longitude is selected by carrying out trial runs in order to obtain an elevated landing point so as to demonstrate the difficulties of landing in most of the regions in the southern hemisphere [1]. Some results of the simulations are given in Table 7. Note that parachute deployment

Table 5. Results of simulations with terminal descent thrusting

| Parameter/Thrust | 17 kN | 18 kN |
|---------------------------------|--------|--------|
| Burn start altitude (m) | 48.80 | 45.99 |
| Burn start time (s) | 254.32 | 254.37 |
| Burn start velocity (m/s) | 60.98 | 60.98 |
| Burn time (s) | 1.61 | 1.52 |
| Velocity impulse achieved (m/s) | 64.32 | 64.33 |
| Propellant mass used (kg) | 6.51 | 6.50 |
| Burnout altitude (m) | 0.05 | 0.08 |
| Burnout velocity (m/s) | 0.55 | 0.32 |
| Touchdown velocity (m/s) | 0.82 | 0.84 |
| Touchdown time (s) | 256.00 | 256.03 |

Table 6. Comparison of simulations with spherical gravity and non-spherical gravity

| Touchdown parameter | Spherical gravity | Non-spherical gravity |
|---|-------------------|-----------------------|
| Longitude (deg.) | 328.89 | 328.90 |
| Latitude (deg.) | 19.83 | 19.83 |
| Velocity (m/s) | 60.87 | 60.85 |
| FPA (deg.) | -89.62 | -89.71 |
| Flight azimuth (deg.) | 213.01 | 224.68 |
| Integrated heat load (J/cm ²) | 4120.08 | 4120.03 |
| Flight time (s) | 255.06 | 255.12 |
| Ground track (km) | 583.15 | 583.18 |

Table 7. Comparison with topographical considerations

| Touchdown Parameters | Nominal | Southern hemisphere |
|---|---------|---------------------|
| Altitude (km) | -3.61 | 2.73 |
| Radial distance (km) | 3389.77 | 3395.25 |
| Longitude (deg.) | 328.44 | 298.89 |
| Latitude (deg.) | 19.68 | -25.66 |
| Velocity (m/s) | 59.60 | 66.89 |
| FPA (deg.) | -89.86 | -86.68 |
| Flight azimuth (deg.) | 126.94 | 258.09 |
| Integrated heat load (J/cm ²) | 4160.69 | 4180.74 |
| Flight time (s) | 320.72 | 218.57 |
| Ground track (km) | 609.09 | 619.81 |

altitude, heat-shield release altitude, etc. are considered w.r.t the Mars areoid and not Mars' surface, for obvious reasons.

The landing elevation (altitude) is negative in the northern hemisphere and is positive in the southern hemisphere. Hence, the touchdown velocity is about 7 m/s higher in the southern hemisphere case. If a soft landing is to be achieved in this case, the thruster must provide this extra 7 m/s velocity impulse. The FPA also has not become close to vertical in the southern hemisphere case. This increases the chance of toppling of the vehicle on touchdown. Again, the flight time is about 100 s lower in the southern hemisphere case. This reduction gives lesser time for the parachute to stabilize and for the thrusting and other systems to initialize, which will bear heavily on the overall system design.

4. ENTRY MISSION DESIGN ANALYSIS

The parameters like peak heat flux, peak dynamic pressure and integrated heat load increase as the ballistic coefficient increases. Peak acceleration decreases with an increase in ballistic coefficient. These are depicted in Figure 4. The simulations are done without heat shield release or parachute deployment as either of these could change the ballistic coefficient drastically. It was also noted that when the ballistic coefficient is higher than 100 kg/m², the parachute deployment Mach number, i.e., the Mach no. at an altitude of 8.6 km becomes above 2. For ballistic coefficients of the magnitude of 250 kg/m², the parachute deployment Mach number reaches close to 10 which makes soft landing of massive entry modules really challenging.

Increased lift will not have much effect on the touchdown velocity but the time taken and the ground track increase much and can be employed if the entry body is to be steered for greater distance. Also, lifting entry reduces all the peak parameters. However, the integrated heat load will rise because of the

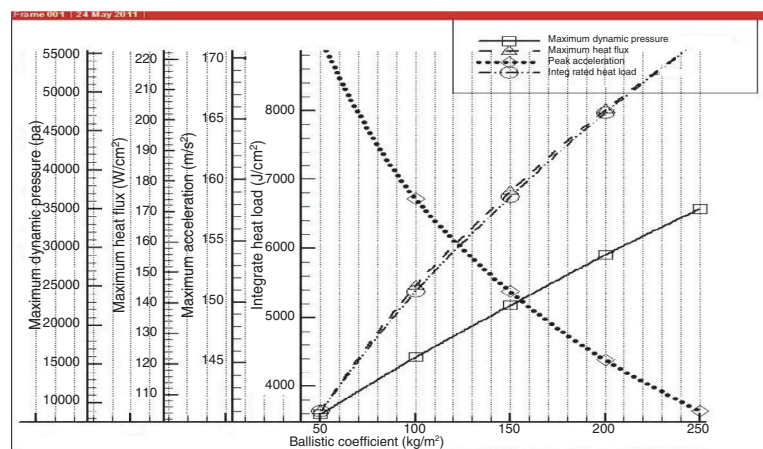


Figure 4. Design chart w.r.t ballistic coefficient.

increase in flight time. These results are illustrated in Figure 5. An increased L/D ratio will decrease the parachute deployment Mach number (at 8.6 km altitude), i.e. the parachute can be deployed earlier if required.

Changing the parachute deployment altitude will have no effect on the peak parameters as they occur at a much higher altitude. But, the flight time, ground track and integrated heat load changes (Figure 6). It also has little effect on touchdown velocity and flight path angle.

An increase in parachute drag coefficient and the parachute diameter have the same effects as both of these changes tend to increase the drag acting on the entry body after the parachute is deployed. A combination of these can bring down the touchdown velocity but the peak parameters like peak dynamic pressure, peak acceleration and peak heat flux on the body cannot be changed. Even though the total time for flight increases as either of these are increased, the integrated heat load decreases slightly due to better deceleration of the module (lower velocity implies lower integrated heat load).

It was observed that all peak parameters as well as integrated heat load increased monotonically with increase in the entry velocity (all other entry parameters remaining the same). A similar trend was observed in the case of entry flight path angles too. A steeper flight path angle inevitably resulted in increased peak parameters. However, integrated heat load decreased when entry was made steeper, probably resulting from shorter flight times for steeper entries.

A purely ballistic entry trajectory may not satisfy the mission requirements of an entry module. In such cases, some kind of active aerodynamic control that adjusts the orientation of the body, and hence its AOA and bank angle, is essential. Since deceleration thrusters cannot be used in the supersonic

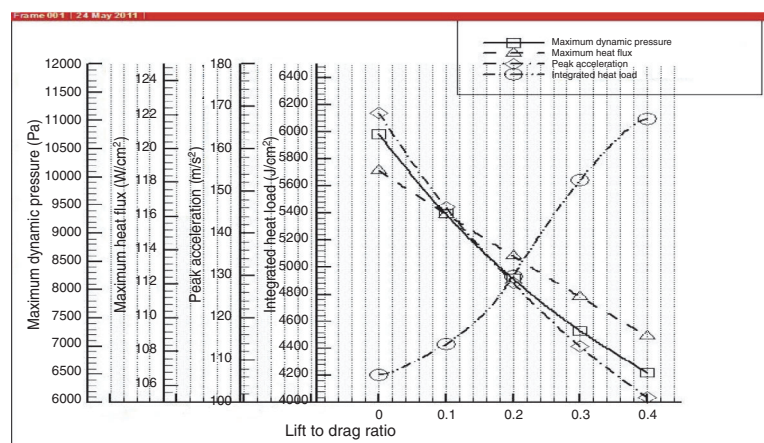


Figure 5. Design chart w.r.t lift to drag ratio.

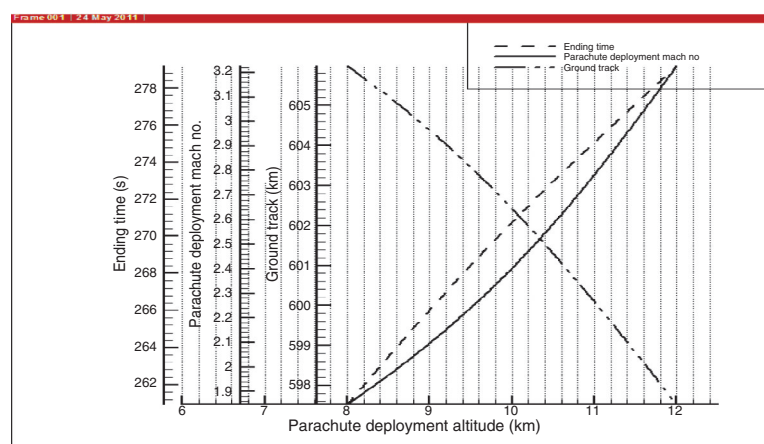


Figure 6. Analysis chart w.r.t parachute deployment altitude.

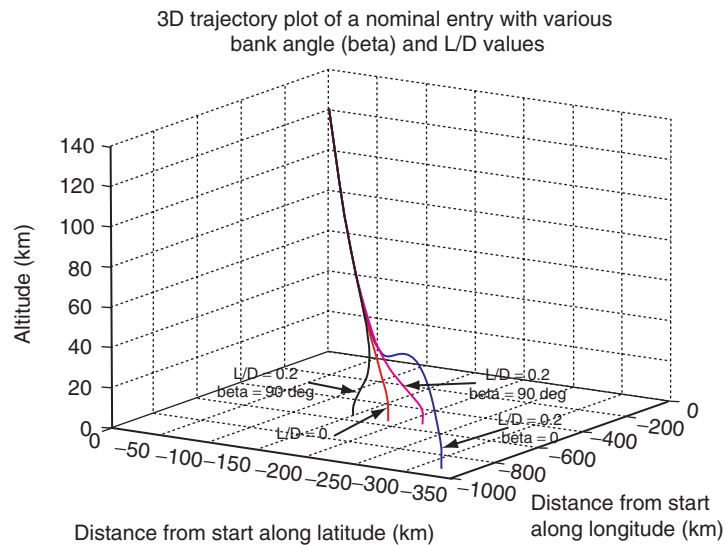


Figure 7. Comparison of entry trajectories with different bank angles and lift to drag ratios.

Mach numbers encountered during the initial phases of entry, the only way out is to rely on aerodynamic control using AOA and bank angle controls.

Optimal control techniques can provide us with the best AOA and bank angle time history so as to achieve the required landing parameters under certain specified constraints. Here, we have carried out a trajectory sensitivity study by varying L/D ratio (basically AOA) and bank angle. Two sets of simulations were carried out, one with $L/D = 0.1$, and the other with $L/D = 0.2$. In each case constant bank angle simulations were carried out for bank angles from -90° to $+90^\circ$.

Looking at the results of the simulations, it is clear that the effect of having a bank angle is predominant only during the latter part of the flight. This would imply that there is not much use in utilising bank angle control in the early stages of entry. Also, we can see that the effects of bank angle control are augmented by having a greater L/D ratio, i.e. a greater AOA for the vehicle. Some of these results are illustrated in Figure 7. The ending ground track, as well as the flight time decreases significantly by the introduction of bank angle control. This also translates to lower integrated heat loads for the entire flight. However, there are also many downsides to having high bank angles, like the increase in peak acceleration, peak heat flux and peak dynamic pressures during entry. Also, bank angle control results in much higher velocities at lower altitudes. There is negligible effect of bank angle control on touchdown velocities and flight path angles.

5. ANALYSIS OF MARS DIRECT ENTRY SCENARIOS WITHIN A LAUNCH WINDOW

Minimum energy Mars mission opportunities occur in every 25 months. For 2013 Mars mission opportunity, energy requirement at Earth Departure is depicted in Figure 8. In general, launch window of an opportunity opens and closes few days before and after the minimum energy epoch. Within a launch window, the arrival hyperbolic trajectory characteristics vary. The arrival characteristics, represented by arrival hyperbolic excess velocity, right ascension and declination results in different entry conditions within a launch window in case of a direct entry, which finally affect the landing spot, and several other atmospheric entry trajectory parameters. Here, a typical launch window in 2013 is analyzed so as to obtain the sensitivity of entry trajectory parameters to the change in departure date within a launch window. The Earth parking orbit in this case is a 250×22800 km with an inclination of 18° w.r.t Earth's equator. The optimal departure date, considering departure velocity impulse as the parameter, is 2013/12/11. Variations resulting from departure 20 days before this date and 10 days after this date are studied.

The entry/initial conditions resulting from these departure dates are computed and are given in Table 8 (velocity vector is w.r.t Mars surface, as per the requirements of the 3D dynamics model). Table 9 shows the key trajectory parameters for entries resulting from departures 20 days prior to 10 days after

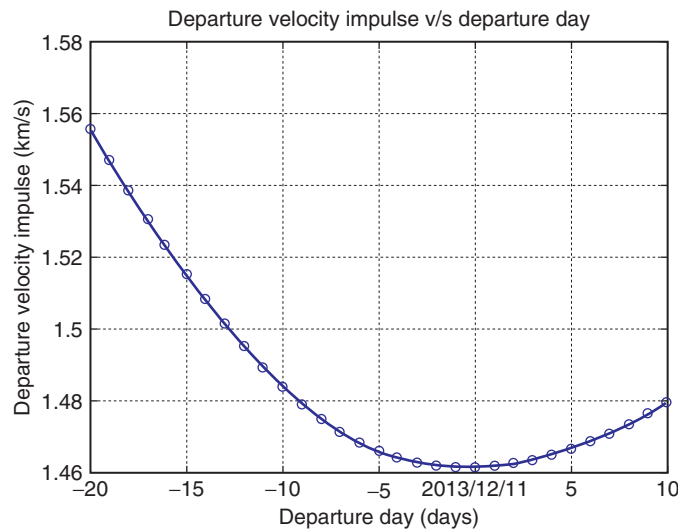


Figure 8. Variation in departure velocity impulse w.r.t departure date.

Table 8. Entry parameters w.r.t departure date

| Departure date | 20 days prior | 10 days prior | 5 days prior | 2013/12/11 | 5 days after | 10 days after |
|-----------------------|---------------|---------------|--------------|------------|--------------|---------------|
| Altitude (km) | 125.90 | 126.04 | 126.10 | 125.80 | 125.11 | 125.27 |
| Longitude (deg.) | 267.69 | 358.52 | 44.09 | 89.87 | 135.95 | 182.35 |
| Latitude (deg.) | -4.52 | -0.13 | 1.91 | 3.75 | 5.34 | 6.75 |
| Velocity (m/s) | 5716.01 | 5719.70 | 5739.70 | 5773.66 | 5822.55 | 5886.65 |
| FPA (deg.) | -12.57 | -12.58 | -12.60 | -12.63 | -12.64 | -12.71 |
| Flight azimuth (deg.) | 152.02 | 152.13 | 152.11 | 152.04 | 151.94 | 151.83 |

Table 9. Trajectory parameters w.r.t departure date

| Departure date | 20 days prior | 10 days prior | 5 days prior | 2013/12/11 | 5 days after | 10 days after |
|---|---------------|---------------|--------------|------------|--------------|---------------|
| Touchdown longitude (deg.) | 273.44 | 4.14 | 49.66 | 95.41 | 141.44 | 187.84 |
| Touchdown latitude (deg.) | -14.92 | -10.55 | -8.50 | -6.63 | -4.97 | -3.53 |
| Touchdown velocity (m/s) | 58.71 | 58.97 | 59.09 | 59.21 | 59.31 | 59.40 |
| Touchdown FPA (deg.) | -89.67 | -89.65 | -89.64 | -89.63 | -89.63 | -89.62 |
| Touchdown flight azimuth (deg.) | 123.59 | 127.08 | 128.61 | 129.95 | 131.07 | 131.99 |
| Integrated heat load (J/cm ²) | 2739.52 | 2740.85 | 2757.81 | 2786.95 | 2829.17 | 2886.04 |
| Flight time (s) | 320.36 | 320.05 | 319.44 | 318.17 | 316.22 | 314.55 |
| Touchdown ground track (km) | 701.97 | 700.96 | 700.03 | 697.16 | 692.23 | 690.63 |
| Peak acceleration (Earth g's) | 8.59 | 8.61 | 8.67 | 8.78 | 8.95 | 9.17 |
| Peak dynamic pressure (kPa) | 5.38 | 5.39 | 5.43 | 5.50 | 5.60 | 5.74 |
| Peak heat flux (W/cm ²) | 49.32 | 49.46 | 50.01 | 50.95 | 52.31 | 54.16 |
| Parachute deployment mach no. | 1.79 | 1.79 | 1.78 | 1.78 | 1.78 | 1.78 |

the optimal departure date. Design limits on each of the design parameters, such as peak acceleration, can be set based on this analysis for a launch window. Subsystems of the entry module can be designed to satisfy the worst requirements within the launch window.

Change in velocity, flight path angle and flight azimuth at touchdown and parachute deployment Mach no. are marginal w.r.t change in departure date. Integrated heat load, peak heat flux, peak

dynamic pressure and peak acceleration increase monotonically from -20 days to $+10$ days of departure date. Departing at a later date will strain the structural and thermal systems of the entry module. However, departure at an earlier date will cause a penalty in the form of increased departure velocity impulse (Figure 8). Thus, all these factors have to be taken into consideration while fixing the departure date.

6. CONCLUSIONS

3D trajectory simulation tool for Mars entry has been developed in C++, and various cases of entry have been analysed and validated using the data available from previous Mars missions (MPF). Various design parameters associated with entry trajectory design are analysed using the tool.

The fact that purely ballistic entry systems with ballistic coefficients greater than 50 cannot be decelerated to sufficiently low speeds below 10 km altitude is clearly visible. Use of lifting entry bodies, supersonic parachutes and/or terminal descent thrusters, is required for smooth landing. Larger ballistic coefficients result in larger peak parameters, which put pressure on material selection for the entry module thermal system and structure. It is observed that bank angle modulation is an effective way of steering the trajectory and adjusting the landing zone. There is a smooth variation in the change of touchdown latitude and longitude, with the change in entry latitude and longitude, which makes the trajectory design process much simpler. For entry trajectories, the effects of non-spherical gravity components are negligible. The necessity of incorporating Mars topography data into the simulations (for accurate landing spot determination) is established.

It has been demonstrated that change in departure date of a Mars entry mission (within a launch window) can vastly change the landing location, and can also affect the design parameters to a certain extent. Also, it is observed that the departure date that is selected based on entry trajectory parameters need not be minimum energy departure date itself.

ACKNOWLEDGEMENTS

We thank Dr. K. S. Dasgupta, Director, IIST, Dr. V. Adimurthy, Dean (R & D), IIST and Prof. Kurien Issac, HOD, Department of Aerospace, for giving us the opportunity to work on this project in IIST.

REFERENCES

- [1] Robert D. Braun, Robert M. Manning, "Mars Exploration Entry, Descent, Landing Challenges", IEEEAC paper #0076, FINAL, Updated December 9, 2005.
- [2] L. Sehnal, "Analytical Models of Mars' Atmosphere Density", Bull. Astron. Inst. Czechosl., Vol. 41 (1990), No. 2.
- [3] Francisco Gonz'alez-Galindo et al, "The Martian Upper Atmosphere", LNEA III, 2008.
- [4] Robert D. Braun, John A. Dec, "An Approximate Ablative Thermal Protection System Sizing Tool for Entry System Design", 44th AIAA Aerospace Sciences Meeting and Exhibit, 9–12 January 2006, Reno, Nevada.
- [5] M. E. Tauber, K. Sutton, "Stagnation-Point Radiative Heating Relations for Earth and Mars entries", JOURNAL OF SPACECRAFT AND ROCKETS, Vol. 28, No. 1, January-February 1991.
- [6] David A. Spencer, Robert D. Braun, "Mars Pathfinder Atmospheric Entry-Trajectory Design and Dispersion Analysis", JOURNAL OF SPACECRAFT AND ROCKETS, Vol. 33, No. 5, September-October 1996.
- [7] "Atmospheric Re-entry Trajectory Optimization with SOCS", public domain document.
- [8] www.grc.nasa.gov
- [9] William H. Press, et al, "Numerical Recipes in C++", Cambridge University Press Pvt. Limited, 2007.
- [10] Runge-Kutta methods' algorithms - "<http://mymathlib.webtrellis.net>".
- [11] Robert D. Braun, Richard W. Powell, Walter C. Engelund, Peter A. Gnoffo, K. James Weilmuenster, Robert A. Mitcheltree, "Mars Pathfinder Six-Degree-of-Freedom Entry Analysis", JOURNAL OF SPACECRAFT AND ROCKETS, Vol. 32, No. 6, November-December 1995.